



**HAL**  
open science

## Mobility of Low Angle Grain Boundaries in Pure Metals

Myrjam Winning, Anthony Rollett, Günter Gottstein, Lasar Shvindlerman, D J Srolovitz, Adele Lim

► **To cite this version:**

Myrjam Winning, Anthony Rollett, Günter Gottstein, Lasar Shvindlerman, D J Srolovitz, et al.. Mobility of Low Angle Grain Boundaries in Pure Metals. *Philosophical Magazine*, 2010, 90 (22), pp.3107-3128. 10.1080/14786435.2010.481272 . hal-00599235

**HAL Id: hal-00599235**

**<https://hal.science/hal-00599235>**

Submitted on 9 Jun 2011

**HAL** is a multi-disciplinary open access archive for the deposit and dissemination of scientific research documents, whether they are published or not. The documents may come from teaching and research institutions in France or abroad, or from public or private research centers.

L'archive ouverte pluridisciplinaire **HAL**, est destinée au dépôt et à la diffusion de documents scientifiques de niveau recherche, publiés ou non, émanant des établissements d'enseignement et de recherche français ou étrangers, des laboratoires publics ou privés.



### Mobility of Low Angle Grain Boundaries in Pure Metals

Journal:	<i>Philosophical Magazine &amp; Philosophical Magazine Letters</i>
Manuscript ID:	TPHM-10-Feb-0056.R1
Journal Selection:	Philosophical Magazine
Date Submitted by the Author:	23-Mar-2010
Complete List of Authors:	Winning, Myrjam; Max-Planck Institute für Eisenforschung GmbH, Microstructure physics and metal forming Rollett, Anthony; Carnegie Mellon Univ., Department of Materials Sci. & Eng. Gottstein, Günter; RWTH Aachen, Institut für Metallkunde und Metallphysik Shvindlerman, Lasar; RWTH Aachen, IMM; Institute of Solid State Physics Russian Academy of Sciences Srolovitz, D J; Agency for Science, Technology and Research, Institute of High Performance Computing Lim, Adele; Princeton University
Keywords:	dislocation interactions, grain boundaries, mobility
Keywords (user supplied):	low angle grain boundaries



## Mobility of Low Angle Grain Boundaries in Pure Metals

M. Winning<sup>1,5</sup>, A.D. Rollett<sup>1</sup>, G. Gottstein<sup>2</sup>, D.J. Srolovitz<sup>6</sup>, A. Lim<sup>3</sup> and L.S. Shvindlerman<sup>2,4</sup>

<sup>1</sup>Carnegie Mellon University, Pittsburgh PA 15213, USA

<sup>2</sup>Institut für Metallkunde und Metallphysik, RWTH Aachen, 52056 Aachen, Germany

<sup>3</sup>Princeton University, NJ 08544, USA

<sup>4</sup>Institute of Solid State Physics, Russian Academy of Science, Chernogolovka, Moscow distr., 142432 Russia

<sup>5</sup>Max-Planck Institute for Iron Research GmbH, 40237 Düsseldorf, Germany

<sup>6</sup>Agency for Science, Technology and Research, Institute of High Performance Computing, Singapore.

### Abstract

The mobility of low angle grain boundaries in pure metals is reviewed and several theoretical treatments are provided. The approach that provides the best agreement with the available experimental data is one in which the mobility is controlled by vacancy diffusion through the bulk to (and from) the dislocations that comprise the boundary that are bowing out between pinning points. The pinning points are presumed to be extrinsic dislocations swept into the boundaries or grown in during the prior processing of the material. This approach yields a mobility that is constant with respect to misorientation angle, up to the transition to the high angle regime. For small misorientations of the order  $1^\circ$ , however, the mobility appears to increase with decreasing misorientation angle.

### Introduction

#### *Background*

The kinetic properties of grain boundaries remain a challenge despite many years of research. In particular, grain boundary mobility is poorly understood even though the broad outline of the physical basis of this property is known [1,2]. An improved understanding would be useful for a very wide range of processing applications. Grain

1  
2  
3 boundaries can be usefully divided into low angle (LAGB) and high angle (HAGB) types,  
4 based on whether or not their structure consists of discrete lattice dislocations. The  
5 relatively simple structure of low angle boundaries permits exploration of the relationship  
6 between boundary structure and boundary mobility.  
7  
8  
9

10 LAGBs are interfaces between crystals (grains) with small enough misorientations that  
11 they comprise a set of discrete dislocations. The dislocation density in a LAGB depends on  
12 the magnitude of the Burgers vector(s) of the dislocations, the magnitude of the  
13 misorientation, and to a lesser extent, on the rotation axis [3]. The variation in LAGB  
14 energy with misorientation angle and axis is well described by the Read-Shockley theory  
15 [4]. Despite the well-defined structure of such boundaries, there is no consensus on how to  
16 describe their mobility quantitatively. This paper reviews the extant LAGB mobility data  
17 and presents a basic theory for describing this important property.  
18  
19  
20  
21  
22  
23  
24

25 LAGB migration can be described in terms of the motion of the constituent dislocations.  
26 Two limiting cases for the rate-controlling step of LAGB migration can be distinguished.  
27 The first is the conservative dislocation motion limit, i.e. that dislocations move by glide.  
28 The second is the dislocation climb limit. The evidence reviewed here points clearly to the  
29 dominance of climb control. Therefore, the theory presented here is based upon non-  
30 conservative dislocation motion.  
31  
32  
33  
34  
35  
36  
37

38 We first identify which feature of the boundary structure is responsible for controlling the  
39 rate of boundary migration. Then we compute the kinetics of the process by which this  
40 feature moves. Assuming that boundary mobility is an intrinsic property, the central  
41 feature of the boundary structure is the set of dislocations that is required to satisfy the  
42 lattice misorientation between grains, taking account of the plane of the boundary<sup>†</sup>.  
43 However, it is also possible that the rate limiting feature in LAGB migration is extrinsic  
44 and related dislocations in the boundary plane that are in excess of those needed to account  
45 for the lattice misorientation. Accordingly we define extrinsic dislocations in a LAGB as  
46 those for which the total Burgers vector per boundary area sums to zero. The distinction  
47  
48  
49  
50  
51  
52  
53  
54

55  
56  
57 <sup>†</sup> We only consider configurations that would not change significantly under applied shear  
58 stress; we also neglect those that would rearrange significantly through climb.  
59  
60

1  
2  
3 between these two is important since it will affect the nature of the dependence of the  
4 mobility on misorientation. Similarly, given the importance of climb, identification of the  
5 diffusion path (and how it depends on grain boundary crystallography and grain boundary  
6 structure) is key. We now consider several approaches to describing LAGB mobility.  
7  
8  
9

10 Dislocation glide was proposed to be the dominant migration mechanism in the analysis of  
11 the classical experiments on zinc [5,6]. In these experiments, stress was used to drive the  
12 migration of low angle ( $\theta < 2^\circ$ ) symmetrical tilt grain boundaries in Zn bicrystals. In order  
13 to move the grain boundaries, stresses of the order of the critical resolved shear stress were  
14 required. The accompanying macroscopic shape changes were compatible with the shear  
15 strain produced by dislocation glide.  
16  
17  
18  
19  
20

21 The activation energy for the migration of LAGBs is comparable to that for self-diffusion  
22 over a wide temperature range [7-9]. By contrast, the effective activation energy for plastic  
23 deformation [10], although similar to that for diffusion at high temperatures, drops to  
24 substantially lower values at low temperatures. This suggests that dislocation glide and  
25 LAGB migration kinetics have different origins. Consideration of the structure of LAGBs  
26 provides an additional argument that suggests that dislocation glide and LAGB migration  
27 have different origins. LAGBs are typically made up of dislocations with two or more  
28 different Burgers vectors. Such dislocations commonly react to form a dislocation network  
29 in which some segments are sessile [11]. The motion of such a boundary requires changes  
30 in the dislocation network structure. This would necessarily produce a barrier for migration  
31 that exceeds that for self-diffusion.  
32  
33  
34  
35  
36  
37  
38  
39  
40  
41

42 Winning, *et al.*, also Molodov *et al.* have performed a series of experiments in which grain  
43 boundary migration was driven by an applied stress [8, 9, 12-14]. They reported  
44 measurements of grain boundary mobility in pure Al for both low and high angle planar  
45 grain boundaries. Figure 1a shows activation enthalpies for migration versus  
46 misorientation for boundaries with  $\langle 100 \rangle$ ,  $\langle 111 \rangle$  and  $\langle 112 \rangle$  misorientation axes. The  
47 enthalpy is constant in both the LAGB and in the HAGB regime for each series but the  
48 angle at which the transition occurs from LAGB (higher enthalpy) to HAGB (lower  
49 enthalpy) behavior is smaller for the  $\langle 100 \rangle$  series. The pre-exponential term in the  
50 mobility is also constant over the same range of angles but shows the opposite change from  
51 low to high, going from LAGB to the HAGB range. Therefore, the mobilities of LAGBs  
52  
53  
54  
55  
56  
57  
58  
59  
60

1  
2  
3 are lower than those for HAGBs at low temperatures (Fig. 1b), in conformance with other  
4 observations, whereas at high temperatures, LAGBs exhibit higher mobilities than HAGBs  
5 (Fig. 1c). The stresses that were used to provide the driving force for motion were  
6 significantly less than the yield stress at the test temperature. In contrast to the Zn bicrystal  
7 experiments, no macroscopic strains were observed in these experiments in Al.  
8 Consequently, the shape change that accompanies dislocation motion must be  
9 accommodated by some other means.

10  
11 The dependence of LAGB mobility on misorientation angle also provides useful hints as to  
12 the LAGB migration mechanism. The experiments in Zn showed that the boundary  
13 migration rate decreased with increasing misorientation angle [5,6]. By analyzing  
14 curvature driven boundary migration in a recrystallized Al foil, Yang, *et al.* also showed  
15 that the LAGB mobility was lower for small misorientations (below approximately 10°)  
16 than for high angle boundaries [15]. In these experiments and those by Winning *et al.*, the  
17 mobility was found to be nearly misorientation-independent at low misorientations. Huang  
18 and Humphreys extracted the misorientation dependence of LAGB mobility from  
19 measurements of subgrain coarsening in single crystals of aluminum [2]. Their results can  
20 be summarized as showing a sharp (power law) increase in mobility with misorientation in  
21 the range 2-6°, with a leveling-off to a slowly increasing mobility above 6°. Although this  
22 suggests a conflict with the results of Winning *et al.* in terms of the misorientation over  
23 which the transition from LAGB to HAGB behavior occurs, the two experiments were  
24 quite different. In particular, the Winning *et al.* results were obtained for nearly symmetric,  
25 individual boundaries with defined crystallography, whereas the Huang and Humphreys  
26 mobility results were inferred from subgrain coarsening rates where misorientation was  
27 defined as the average misorientation of a given (sub)grain with all of its neighbors. Furu  
28 *et al.* also studied subgrain coarsening kinetics by measuring recovery rates in a  
29 commercial purity aluminum [16]. They concluded from the high activation energy  
30 (~ 175 kJ/mole) and the magnitude of the activation volume that LAGB migration was  
31 dominated by solute drag of dissolved iron [1,17].

32  
33 The similarity of the behavior of the LAGB mobilities in several systems suggests that  
34 LAGB migration is incompatible with dislocation glide control, and that LAGB migration  
35 is controlled by dislocation climb. In the following sections, we analyze LAGB mobility in  
36 terms of the climb of the dislocations in the boundary and compare the predictions with the  
37  
38  
39  
40  
41  
42  
43  
44  
45  
46  
47  
48  
49  
50  
51  
52  
53  
54  
55  
56  
57  
58  
59  
60

experimental results. We consider both pure low angle tilt boundaries with only parallel edge dislocations and more general boundary types with a twist component or with extrinsic dislocations. Note that we do not attempt to explain or model the transition from low- to high-angle behavior.

## THEORETICAL ANALYSES

### 2.1 Driving Force

In this section we investigate the mobility of flat boundaries and begin by defining the driving force for migration. Consider, for simplicity, a symmetrical boundary with a [112] tilt axis in an fcc material, Fig.2a. This LAGB is made up of perfect crystal dislocations each with a Burgers vector  $\mathbf{b} = \frac{a}{2}[1\bar{1}0]$  each lying in a  $(11\bar{1})$  glide plane, Fig.2a. The following expression relates the spacing between the edge dislocations  $d$ , the rotation angle  $\theta$ , and the magnitude of the Burgers vector  $b$ :

$$\frac{b}{2d} = \sin \frac{\theta}{2} \quad (1a)$$

which, for small angles can be approximated as

$$d = b/\theta. \quad (1b)$$

Note that in this case, the Burgers vectors are orthogonal to the boundary plane.

When a shear stress  $\tau$  is applied to the boundary, each dislocation experiences a force  $F^s$ , perpendicular to its line element  $\xi$  and the component perpendicular to the boundary is then given by the Peach-Koehler-equation [18]

$$F_x^s = [(\boldsymbol{\sigma} \cdot \mathbf{b}) \times \boldsymbol{\xi}]_x = \tau b \cos(\theta/2) \quad (2)$$

The force on the boundary, per unit area, is related to the planar density of dislocations  $\rho_s = 1/d$  and, hence, to the misorientation angle  $\theta$  through Eq. (1a),

$$p = F_x^s \rho_s = F_x^s \frac{1}{d} = \tau \sin \theta \approx \tau \theta \quad (3)$$

This model is appropriate for zinc, where stress-driven boundary migration occurs at the yield stress (i.e., dislocation glide-control) [5,6]. We recall, however, that in other materials, the experimental observations suggest that the mobility of symmetric LAGBs is



1  
2  
3 diffusion-controlled. Note that LAGBs can also migrate under a capillary driving force,  
4 which, however, we do not address here [19].  
5  
6  
7

## 8 9 2.2 Diffusional Climb of Extrinsic Dislocations

10  
11 We have pointed out above that a perfect symmetric tilt grain boundary should be able to  
12 move by dislocation glide under an imposed shear stress when the Peierls stress of the  
13 dislocations is exceeded. The Peierls stress of perfect dislocations in fcc crystals is very  
14 low and one might expect that LAGBs in fcc metals should offer the best chance of  
15 observing such behavior. We must consider the role of extrinsic dislocations in LAGBs,  
16 however, and the possibility that they control the mobility. Since such dislocations belong  
17 to slip systems other than that of the structural dislocations of the grain boundary, they  
18 have to climb if they are to remain with the moving boundary. The net Burgers vector of  
19 all redundant or extrinsic dislocations must be zero, otherwise the character of the  
20 boundary would be changed. We assume that the extrinsic dislocations lie in the boundary  
21 plane and that there are equal numbers with opposite sign. The spacing of these antiparallel  
22 dislocations is random but on average  $\lambda \approx 1/\sqrt{\rho_R}$ , where  $\rho_R$  is the redundant dislocation  
23 density. We further assume that the extrinsic spacing  $\lambda$  is independent of misorientation  
24 because they arise from faults in growth processes, or sweeping up of dislocations during  
25 migration, not from the geometric nature of the boundary. Note also that the motion of the  
26 extrinsic dislocations allows for balanced exchange of vacancies between (only) the  
27 (extrinsic) dislocations of opposite sign.  
28  
29  
30  
31  
32  
33  
34  
35  
36  
37  
38  
39  
40  
41

42 Another possible source of extrinsic dislocations concerns the constraints on experiments  
43 on LAGB mobility. It is important to note that the experiments performed by Winning *et*  
44 *al.* [8,9] did not give rise to any macroscopic (shear) displacements in the vertical direction  
45 (y-direction in Fig.2). Such displacements are a direct geometrical consequence of  
46 collective motion of the intrinsic dislocations of a tilt grain boundary, as shown in the  
47 experiments on Zn [5,6]. This means that some type of accommodation must have been  
48 made within the sample in order for the boundaries to move without causing shear strains.  
49 This will be discussed further in a subsequent publication but could, for example, be  
50 accommodated by additional dislocations crossing the interface as it moves in order to  
51 offset the strain associated with the motion of the intrinsic dislocations. Such a secondary  
52  
53  
54  
55  
56  
57  
58  
59  
60



dislocation motion might become much easier in boundaries whose dislocation spacing is less than a critical spacing.

If one considers the driving force from an applied stress on the extrinsic dislocations, one can consider the force to be transmitted through the Peach-Koehler force on the intrinsic dislocations, which in turn interact with the extrinsic (redundant) dislocations. This is equivalent to making the assumption that all the available energy is dissipated in moving the extrinsic dislocations and none in moving the intrinsic dislocations. This gives rise to a climb force,  $F^s$ , on the extrinsic dislocations in the  $x$ -direction,

$$F_x^s = \tau b \cos(\theta/2). \quad (4)$$

The driving force is then exactly as given in Eq. 3. Redundant dislocations of opposite sign must climb in opposite directions in order to remain with the moving boundary, Fig. 3.

Thanks to their equal and opposite numbers, this can be accomplished by vacancy exchange. The corresponding diffusion flux,  $J$ , can be written as

$$J = -\frac{D_L}{\Omega kT} \frac{d\mu}{dy} = -\frac{D_L}{\Omega kT} \frac{2\tau\Omega}{\lambda} \quad (5)$$

where  $D_L$  is the atom diffusivity in the lattice,  $\mu$  is the chemical potential,  $kT$  is the thermal energy and  $\Omega$  is an atomic volume. Note that the gradient of the chemical potential  $\mu$  is simplified to a gradient parallel to the boundary wall and dependent on the spacing,  $x$ , of the extrinsic dislocations. The flux passes through a cross section  $\delta b$  where  $\delta$  is the width of the diffusion zone perpendicular to the boundary, effectively the thickness of the boundary. Every atom transferred will move the dipolar arrangement of related redundant dislocations by an atomic spacing  $b$  so that the corresponding velocity is:

$$v = Mp = M \cdot \tau\theta = b\delta b \frac{D_L}{\Omega kT} \frac{2\tau\Omega}{\lambda} = \frac{2\delta b^2 D_L}{\lambda kT} \tau \equiv \frac{C D_L}{\lambda kT} \tau \quad (6)$$

where  $C$  is defined by this equation as  $C = 2\delta b^2$ ,  $M$  is the grain boundary mobility, and  $p$  is the driving force, as before. If the climbing dislocations are extrinsic dislocations

1  
2  
3 embedded in a symmetric low angle tilt boundary,  $v$  is identical with the velocity of the tilt  
4 boundary since the climb process is rate controlling. As noted in Eq 6, the drift velocity of  
5 the boundary can be expressed as the product of mobility and driving force. Consequently  
6  
7  
8

$$M = \frac{C D_L}{\lambda kT} \frac{1}{\theta} = \frac{2\delta b^2 D_L}{\lambda kT} \frac{1}{\theta} \quad (7)$$

9  
10  
11  
12  
13  
14  
15 It is stressed that  $\lambda$  is independent of the misorientation and, therefore, the grain boundary  
16 mobility is inversely proportional to the misorientation. This the mobility proposed by  
17 Sutton and Balluffi [16] within numerical constants of order unity. A similar derivation  
18 and result was presented by Furu *et al.* [13]. One note of caution is in order here: if a  
19 migrating boundary sweeps up additional extrinsic dislocations then the spacing will  
20 decrease, leading to a decrease in the mobility via Eq. 7 above. Eq. 6 above suggests that  
21 the velocity depends on stress (as it should) but is independent of the misorientation angle.  
22  
23  
24  
25  
26  
27

28 The obvious defect in this theory is that it predicts that the mobility decreases with  
29 increasing misorientation angle whereas experiments show that the mobility of low angle  
30 boundaries tend to be either constant [15] or to increase with increasing misorientation  
31 angle [2]. In all but the most ideal, low angle, tilt grain boundaries that constitute a tiny  
32 fraction of general LAGBs, the dislocation structure is two-dimensional, rather than a  
33 regular array of straight, parallel edge dislocations. Such a two-dimensional structure may  
34 form because (a) the primary dislocations arise from sets of non-parallel slip planes  
35 intersecting the boundary, (b) there are dislocation reactions that lead to low energy  
36 structures, (c) the boundary may have a twist component that provides a two dimensional  
37 array of screw dislocations superimposed upon the edges that account for the tilt  
38 component, or (d) that there are additional extrinsic dislocations present in the boundary.  
39 In a two-dimensional array of dislocations, the flux between adjacent, climbing  
40 dislocations can occur both by lattice diffusion and pipe diffusion, along dislocation cores.  
41 Except at the highest temperatures, the atom flux, and hence the dislocation climb and  
42 boundary migration rate, should be determined by pipe diffusion, which typically exhibits  
43 a much smaller activation energy than for lattice diffusion. Furu *et al.* [16] briefly  
44 considered the possibility that pipe diffusion may play a role in the mobility of low angle  
45 boundaries. In order to address this point we next investigate the effects of pipe diffusion  
46 on the motion of low angle grain boundaries.  
47  
48  
49  
50  
51  
52  
53  
54  
55  
56  
57  
58  
59  
60

### 2.3 Pipe Diffusion Model

Consider the case of a grain boundary containing two sets of dislocations, one parallel to the tilt axis and one perpendicular to it. In order to make a direct analogy with the model described above, we consider that in order for the boundary to migrate, the dislocations parallel to the tilt axis must undergo diffusional climb, while the orthogonal set of dislocations can glide. Such a situation could arise when there is a slight twist component to an otherwise perfect symmetric tilt boundary. The gradient in the chemical potential driving diffusion between the dislocations parallel to the tilt axis is the same as in the lattice diffusion case, described above. However, in the present case, the diffusional flux responding to the chemical potential gradient has two distinct components, through the lattice and along the dislocation lines that run perpendicular to the tilt axis. The lattice contribution is as described in Eq. (5) and the flux along the dislocation lines is

$$J_{\perp} = -\frac{D_{\perp}}{\Omega kT} \nabla \mu, \quad (8)$$

where  $D_{\perp}$  is the diffusivity associated with the cores of dislocations that run perpendicular to the tilt axis. The total current of atoms from one dislocation parallel to the tilt axis to the next (per length of boundary) is

$$I = AJ + J_{\perp} \frac{\pi \delta^2}{d_2} \cong \frac{\tau}{kT} \left( D_L + \frac{\pi D_{\perp} \delta^2}{d_1 d_2} \right), \quad (9)$$

where  $\delta$  is the radius of the fast diffusion pipe at the dislocation core and  $d_1$  and  $d_2$  are the spacings between the dislocations that run parallel and perpendicular to the tilt axis, respectively. The boundary velocity is related to the diffusional current as in Eq. 6 but with contributions from both lattice and pipe diffusion

$$v = I \frac{\Omega}{b} \cong \frac{\Omega}{kTb} \tau \left( D_L + \frac{\pi D_{\perp} \delta^2}{d_1 d_2} \right) \cong \frac{\Omega}{kTb} \left( D_L + \frac{\pi D_{\perp} \delta^2 \theta}{bd_2} \right) \tau. \quad (10)$$

Note that the misorientation angle,  $\theta$ , in this equation refers to the tilt component alone (with  $\theta \approx b/d_1$  for small angles) and that the additional dislocations that lie perpendicular to the axis increase the total misorientation. The mobility  $M = v/(\tau\theta)$  is now simply:

$$M \cong \frac{\Omega}{kTb} \left( \frac{D_L}{\theta} + \frac{\pi D_{\perp} \delta^2}{bd_2} \right). \quad (11)$$

This expression suggests that the mobility increases as the spacing between dislocations perpendicular to the tilt axis decreases. If the density of dislocations running perpendicular to the tilt axis is associated with a twist component, then

$$M \cong \frac{\Omega}{kTb} \left( \frac{D_L}{\theta} + \frac{\pi D_{\perp} \delta^2}{b^2} \phi \right), \quad (12)$$

where  $\phi$  is the twist component of the misorientation. On the other hand, a network of dislocations with line directions running both parallel and perpendicular to the tilt axis may be present even in a pure tilt boundary assuming that dislocation reactions occur. If the density of the perpendicular dislocations is proportional to the density of parallel ones, then the mobility is

$$M \cong \frac{\Omega}{kTb} \left( \frac{D_L}{\theta} + \alpha \frac{\pi D_{\perp} \delta^2}{b^2} \theta \right), \quad (13)$$

where  $\alpha$  is a proportionality factor. This result is similar to that briefly mentioned by Furu *et al.* [16]. One interesting consequence of this approach is that it predicts a breakpoint in an Arrhenius plot of mobility versus reciprocal temperature where the dominant diffusion mode changes from bulk to pipe diffusion.

This result is an improvement on the previous one in that the mobility increases with misorientation at large enough misorientations. Nonetheless, there will always be a range of misorientation over which the mobility is decreasing. The extent of the range depends of course on the relative strengths of the bulk and pipe diffusion terms, as well as the relative dislocation densities. In order to estimate the mobility of low angle boundaries in aluminum, diffusion parameters have been taken from the literature. [20]. Evaluation of Eq. 14 for aluminum at 473K suggests that, to a first approximation, the mobility should decrease in the range 0-5° and then increase again.

#### 2.4 Vacancy exchange between adjacent dislocations: symmetrical low angle tilt boundaries

In contrast to the special case of grain boundaries composed of a single set of geometrically necessary dislocations with the Burgers vector perpendicular to the boundary plane discussed above, more general LAGBs contain sets of dislocations with different Burgers vectors which, except in special cases, are not perpendicular to the grain boundary plane. As Read and Shockley discussed [4], such boundaries cannot move by glide alone.

1  
2  
3 Instead some amount of non-conservative motion is required. Thus Sutton and Balluffi  
4 [21] and others [11,22] noted that the motion of LAGBs will generally involve the  
5 simultaneous glide and climb of the component dislocations (consider the motion of the  
6 dislocation boundary normal to itself, Fig. 4). In order to develop a quantitative model,  
7 Sutton and Balluffi adopted the particular symmetric tilt configuration discussed by Read  
8 and Shockley that comprises two Burgers vectors of equal densities and parallel line  
9 directions, Fig. 4. In the fcc crystal structure, this corresponds, for example, to the case of a  
10 100 misorientation axis and a 001 boundary normal [23]. The key feature of this boundary  
11 type is that vacancies are emitted by one dislocation type and can be absorbed by the other;  
12 see, for example, fig. 8 of [4]. Therefore the production and absorption of vacancies is  
13 balanced within the boundary and the rate of tilt boundary migration (dislocation climb) is  
14 controlled by lattice diffusion between adjacent dislocations. Again, it is emphasized that  
15 this is a special case, and the more general case of unbalanced diffusion will be treated  
16 below.  
17  
18  
19  
20  
21  
22  
23  
24  
25  
26  
27

28 The general expression for the atom flux between the dislocations is:

$$J = -\frac{D_L}{\Omega kT} \nabla \mu, \quad (14)$$

30  
31  
32  
33  
34  
35 where  $D_L$ ,  $\Omega$ ,  $k$  and  $T$  are defined as before (for Eq. 4). A stress,  $\tau$ , that tends to move  
36 dislocations with Burgers vectors perpendicular to the boundary plane, produces a  
37 chemical potential gradient between adjacent dislocations associated with the non-  
38 perpendicular component of the Burgers vector:  
39  
40  
41

$$\nabla \mu \cong \frac{\tau \Omega}{d}, \quad (15)$$

42  
43  
44  
45  
46 where  $d$  is the distance between dislocations in the tilt boundary.

47 The flux of atoms between the dislocations passes through some area (per length of  
48 boundary in a direction parallel to the tilt axis) of the matrix between the dislocations,  
49 which we take to be a constant boundary width,  $\delta$ . The total current of atoms between the  
50 two adjacent dislocations (per length of boundary)  $I$  is  
51  
52  
53  
54

$$I = AJ \cong \frac{\delta D_L \tau}{dkT}. \quad (16)$$

Assuming that the rate of boundary migration is controlled by how fast the dislocations climb, the boundary velocity can be written as the current of atoms to the dislocations (per length of boundary in the direction parallel to the tilt axis) times the distance advanced per dislocation for each atom that arrives, multiplied by the unit length of the boundary:

$$v = I \frac{\Omega}{b} \cong \frac{\delta D_L \Omega}{dkTb} \tau = \frac{\delta D_L \Omega \theta}{kT} \tau . \quad (17)$$

Note that we have assumed that the climb-to-glide ratio is one for simplicity: in general the ratio may be less than one, depending on the geometry of the boundary. The driving force or pressure on the boundary is the product of the Peach-Koehler force on each dislocation times the number of dislocations per unit length,  $\tau\theta$ , as given above. Hence, the boundary mobility is

$$M = \frac{\delta D_L \Omega}{kTb} . \quad (18)$$

Note that this mobility is different from that proposed by Sutton and Balluffi [21] or Furu *et al.* [16], mainly because of the assumption of constant boundary width, within which vacancy diffusion takes place. The mobility is now *independent* of the misorientation. However, the velocity is predicted to *increase* with misorientation angle, Eq. 17, which is the *opposite* of the experimental observations of Li, Bainbridge [5,6].

### 2.5 Asymmetric low angle tilt boundaries

The simplest asymmetric tilt boundary consists of 2 types of edge dislocations, the ratio of which is determined by the deviation from the symmetrical position. The geometry of such boundaries is complicated when  $\langle 110 \rangle$  lattice Burgers vectors appropriate to fcc lattices are used. Even for a  $\langle 111 \rangle$  tilt rotation axis, asymmetric tilt boundaries have two sets of dislocations whose Burgers vectors are such that their line directions cannot both be parallel and lie in their slip planes. Therefore for the purposes of illustration we discuss the simpler case of asymmetric tilt boundaries containing  $\langle 100 \rangle$  Burgers vectors. In an fcc lattice an asymmetric  $[001]$  tilt boundary consists of 2 sets of edge dislocations with Burgers vectors  $[010]$  and  $[100]$ , and line element  $[001]$  and there are 2 symmetrical  $[001]$  boundary positions which are mutually inclined at  $90^\circ$ .

An asymmetrical [001] low angle tilt boundary of misorientation  $\theta$  and inclination  $\psi$  (with regard to the symmetrical boundary composed only of [100] dislocations) is comprised of a mixture of  $n_1$  dislocations of  $\mathbf{b}_1 = b[100]$  and  $n_2$  dislocation of  $\mathbf{b}_2 = b[010]$  (Fig. 5) with

$$n_1 = \frac{1}{d_1} = \frac{\theta \cos \psi}{b_1}, \quad n_2 = \frac{1}{d_2} = \frac{\theta \sin \psi}{b_2} \quad (19)$$

The total dislocation density in the boundary (per unit area) is

$$n_1 + n_2 = \frac{\theta}{b_1} (\cos \psi + \sin \psi) \quad (20)$$

or the average spacing

$$\bar{d} = \frac{1}{n_1 + n_2} = \frac{b_1}{\theta (\cos \psi + \sin \psi)} \quad (21)$$

and the ratio of the two types of dislocations

$$\alpha = \frac{n_1}{n_2} = \cot \psi \quad (22)$$

For a motion of this boundary in [100] direction, dislocations of type  $\mathbf{b}_1$  can move by slip while dislocations of type  $\mathbf{b}_2$  have to climb in order to keep up with the boundary. The vacancies that are required cannot be supplied by extrinsic dislocations because of the high density of climbing intrinsic dislocations. This then is another point of departure from the analyses available in the literature which all assume that balanced exchange of vacancies is possible on a local basis. The vacancy supply has to be generated by bulk sources. If the vacancy concentration in the bulk is in equilibrium, there is a chemical potential difference between bulk and boundary in case of an external stress  $\tau\Omega$ . Since the stress field of a boundary attenuates within a distance  $\bar{d}$  from the boundary, the flux is, by analogy to Eq. (5):

$$J = -\frac{D}{\Omega kT} \frac{\tau\Omega}{\bar{d}} \quad (23)$$



Since each atom transferred will essentially move the boundary by one atomic spacing, the velocity of the boundary becomes:

$$v = Mp = M \cdot \tau\theta = bd_2b \frac{D_L}{\Omega kT} \frac{\tau\Omega}{d} = \frac{b^2 D_L}{kT} \frac{d_2}{d} \tau \quad (24)$$

From this the mobility is given by:

$$M = \frac{D_L b^2}{kT} \frac{\sin\psi + \cos\psi}{\sin\psi} \frac{1}{\theta} \quad (25)$$

In contrast to the case of balanced exchange of vacancies within a boundary considered in 2.4, the mobility decreases with increasing misorientation angle and also decreases with increasing inclination. In the next section, we consider the behavior of a boundary that can bow out between pinning points whose spacing is determined by the extrinsic dislocation content, rather than the intrinsic (structural) dislocations in the boundary. The analysis just given can be repeated for an asymmetric tilt boundary but with the majority dislocations bowing out between the minority dislocations that must climb<sup>1</sup>. The result is essentially the same as in Eq. (28) but with an additional  $\tan(\psi)$  in the denominator.

---

<sup>1</sup> In this section we have tacitly assumed that the boundary is displaced parallel to the Burgers vector  $b_1$ . The velocity of a boundary, however, is by definition the displacement rate perpendicular to the boundary plane, which in an asymmetrical boundary is inclined to  $b_1$ . This is not a problem, however, since dislocations with  $b_1$  will always remain glissile. while dislocations with  $b_2$  will always have to climb as long as  $\psi \leq \frac{\pi}{4}$ . For  $\psi > \frac{\pi}{4}$  the dislocations with  $b_1$  and  $b_2$  change their role as dislocations with  $b_2$  become glissile while those with  $b_1$  have to climb. This does not change the general problem, since one set of dislocations always has to climb and this process is always rate controlling.

## 2.6 Mobility of flexible LAGBs

For high misorientation angles the density of structural dislocations will be much higher than the density of extrinsic dislocations in the grain boundary (Fig. 6). When dislocations are subjected to a non-zero resolved shear stress they will move unless a reaction force builds up and balances out the forward driving force. Equivalently, the structural dislocations in a low angle grain boundary will move upon action of a shear stress, and the boundary will bow out between the pinning points until a force balance is attained (Fig. 6). The force on each pinning point is the sum of all forces by dislocations acting on it through the superposition principle. If there are  $n$  dislocations between adjacent dipolar pinning points, the stress at each pinning point will be  $n\tau$ .

$$n = \zeta \frac{1}{d} = \zeta \frac{\theta}{b}, \quad (26)$$

where  $\zeta$  is the spacing of the pinning points (in the vertical direction), and  $d$  is the spacing of the intrinsic (structural) dislocations, Eq. 1b. Note that the pinning points are assumed to have a constant spacing related to defects in the material other than the boundary itself. The intrinsic dislocations will maintain a nearly constant spacing, which means that the forces on the pinning points are evenly distributed along their lengths. They may be caused by the presence of extrinsic dislocations in which case the pinning center spacing will be comparable to the extrinsic dislocation spacing,  $\zeta \approx \lambda$ . If the pinning points are able to move by climb due to the diffusional exchange of atoms in a potential gradient then,

$$\nabla\mu = \frac{2n\tau\Omega}{\zeta}. \quad (27)$$

The diffusion flux,  $J$ , is given by:

$$J = -\frac{D_L}{\Omega kT} \nabla\mu = -\frac{D_L}{\Omega kT} \frac{2n\tau\Omega}{\zeta} = -\frac{D_L}{\Omega kT} \frac{2\lambda\theta\tau\Omega}{b\zeta} = -\frac{2D_L\theta}{bkT} \tau \quad (28)$$

This diffusion flux will cause a grain boundary velocity

$$v = Mp = M \cdot \tau\theta = J\delta b \cdot b = 2\delta b \frac{D_L}{kT} \theta\tau \quad (29)$$

As before, the boundary mobility is given by

$$M = 2\delta b \frac{D_L}{kT}, \quad (30)$$

so that the boundary mobility is independent of misorientation in this case. This is a new and quite general result for lattice diffusion controlled and stress driven grain boundary motion that stands in contrast to previous analyses [4, 16,21].

This condition is most likely to apply in the case where the intrinsic dislocation density is much higher than that of the extrinsic dislocations. For literature values of the self-diffusion coefficient in aluminum reproduced in Table 1, one obtains the following values listed in Table 2:

Inserting these values into Eq. 30 gives an estimate of the mobility of low angle boundaries in Al of  $4 \mu\text{m} (\text{s.MPa})^{-1}$ . This is one order of magnitude lower than the measured mobility of a  $13^\circ \langle 112 \rangle$  tilt boundary which is about  $60 \mu\text{m} (\text{s.MPa})^{-1}$ . Note that the analysis assumes in effect that one vacancy per dislocation is required to advance the boundary by one atomic distance. In fact, most boundaries will have a smaller climb to glide ratio, as noted by Bauer and Lanxner [23], and thus the actual mobility will be higher than this simple estimate. Therefore the discrepancy is less serious than it might seem.

### 2.7 Pinning of LAGB by Dipolar Extrinsic Dislocations

The interaction between individual dislocations and low angle boundaries has received limited attention, which motivates the presentation of an example of the grain boundary pinning mechanism proposed above. First we note that Li has discussed such interactions with the principal motivation being to understand the role of low angle grain boundaries on plastic strength [24]; the main conclusion was that penetration of a symmetric tilt LAGB

1  
2  
3 by single dislocations occurs at stress levels little different from the interaction between the  
4 moving dislocation and the nearest individual dislocation in the wall.  
5

6  
7 The example of dipole drag of a LAGB is as illustrated in Fig. 7 as a combination of a  
8 symmetric tilt wall with Burgers vector parallel to  $[110]$  and dipolar dislocations with  
9 Burgers vectors parallel (and anti-parallel) to  $[\bar{1}10]$ ; the boundary normal is parallel to  
10  $[110]$  and line direction of the dislocations is  $[\bar{1}\bar{1}2]$ . Both glide and climb motions of the  
11 dislocations are included in the calculation. A shear stress is applied on the  $(\bar{1}11)$  plane in  
12 the  $[110]$  direction so as to move the intrinsic dislocations to the right in the figure. Forces  
13 between the dislocations are calculated using standard linear elastic analysis [25]. A  
14 program was written in Matlab to allow the configuration of the dislocation array to be  
15 repeatedly calculated as the shear stress moves the LAGB. The main results are as follows.  
16  
17 If climb is not allowed, the intrinsic dislocations move short distances under the action of  
18 the shear stress, such that the boundary effectively bows out as illustrated by Fig. 8. If  
19 climb is allowed (with a mobility equal to 0.2 of the glide mobility) and the shear stress is  
20 small (of order  $3 \cdot 10^{-3}$  of the shear modulus) then the dipolar extrinsic dislocations climb so  
21 as to remain in the (moving) boundary. For somewhat higher shear stresses (of order  $4 \cdot 10^{-3}$   
22 of the shear modulus), the boundary escapes from the extrinsic dislocations and the  
23 pinning effect is lost. In summary, this example shows it is possible for dipolar extrinsic  
24 dislocations to exert a pinning effect on a low angle boundary as analyzed in the previous  
25 section. A more detailed analysis is in preparation [25].  
26  
27  
28  
29  
30  
31  
32  
33  
34  
35  
36  
37  
38  
39  
40  
41

## 42 Discussion

43 Table 3 summarizes the various possibilities for rate-controlling mechanisms of LAGB  
44 migration. The first entry is for dislocation glide of a boundary containing a single  
45 dislocation type, i.e. a single Burgers vector. As discussed above, we rejected this  
46 mechanism as incompatible with the observed activation energies. The second entry is for  
47 a general boundary type, which, however, contains extrinsic dislocations, for which climb  
48 of the extrinsic dislocations controls the mobility. The third entry allows for a twist  
49 component, and differs only with respect to "short circuit" diffusion through the network  
50 of dislocations in the boundary. For all of these the misorientation dependence is again  $1/\theta$ ,  
51 although pipe diffusion could lead to lower activation energies, provided that no long-  
52  
53  
54  
55  
56  
57  
58  
59  
60

1  
2  
3 range diffusion is required. In general, however, non-conservative motion of multiple  
4 dislocation types cannot be accomplished without a net flux of vacancies to or from the  
5 boundary. Some analyses in the literature assume that the exchange of vacancies is  
6 balanced such that only local fluxes are required for long-range boundary migration but  
7 this applies to only a very limited set of grain boundary types. The fourth entry is for  
8 migration of a particular boundary type containing equal densities of geometrically  
9 necessary dislocations with two different Burgers vectors. The mobility of such boundaries  
10 is independent of the misorientation angle. The fifth entry considers an asymmetric LAGB  
11 that contains (intrinsic) two Burgers vectors. Although the magnitude of the mobility is  
12 different (lower) than that of a single-Burgers vector (symmetric) boundary type, the  
13 misorientation dependence is still reciprocal. The last (sixth) entry considers a general  
14 LAGB that has to overcome obstacles which are widely spaced in relation to the intrinsic  
15 dislocation spacing: in this case the mobility is independent of the misorientation, as for  
16 the case of climb control from extrinsic dislocations that act as pinning points.  
17  
18  
19  
20  
21  
22  
23  
24  
25  
26  
27  
28  
29

30 The analyses given above reveal that diffusion controlled grain boundary migration always  
31 yields a mobility which decreases with  $1/\theta$  with increasing misorientation where the  
32 migration is controlled by climb of the intrinsic dislocations. The general result,  $M \sim 1/\theta$ , is  
33 due to the fact that the driving force increases with increasing misorientation, since the  
34 number of intrinsic (structural) dislocations also increases with misorientation and thus the  
35 force on the boundary, while the velocity of the climbing dislocations, which controls the  
36 migration rate, is independent of misorientation. On the other hand, if the grain boundary  
37 migration is controlled by climb of extrinsic dislocations or the climb of extrinsic  
38 dislocations (with an approximately constant spacing,  $\lambda$ ) is accomplished by pipe diffusion  
39 along the intrinsic dislocations, or if the intrinsic dislocations can bow out between pinning  
40 points (perhaps resulting from the presence of extrinsic dislocations) then the mobility is  
41 *independent* of misorientation. The experimental evidence on activation energies points,  
42 however, to a bulk diffusion mechanism in most cases which suggests that the mechanism  
43 considered in section 2.6, i.e. bowing out of the intrinsic dislocations between pinning  
44 points, as the most likely mechanism.  
45  
46  
47  
48  
49  
50  
51  
52  
53  
54  
55  
56  
57  
58  
59  
60

1  
2  
3 There are only a very few experimental data with which to compare these calculations. Li  
4 *et al.* reported that the migration rate of low angle boundaries decreased with  
5 misorientation up to an angle of  $2^\circ$  [5]. The associated activation energy was always close  
6 to that of bulk self diffusion. The stresses required to move their boundaries were reported  
7 to be comparable to the critical resolved shear stress at the relevant temperature. They  
8 observed cases in which two migrating LAGBs coalesced: under the same applied shear  
9 stress, the (trailing) boundary with lower misorientation migrated faster and therefore  
10 caught up with the higher misorientation boundary in front of it, suggesting a decrease in  
11 mobility faster than  $1/\theta$ . Similar coalescence events were observed indirectly by Biberger  
12 and Blum in creep experiments in lithium fluoride [26].

13  
14  
15  
16  
17  
18  
19  
20  
21 Most recently, Winning *et al.* investigated stress driven migration of symmetrical and  
22 slightly asymmetrical  $\langle 112 \rangle$  and  $\langle 111 \rangle$  low angle tilt boundaries with tilt angles of  $3.5^\circ$   
23 and above [8,9]. They used stresses well below the critical resolved shear stress for plastic  
24 yield but also found an Arrhenius type temperature dependence of the migration rate with  
25 an activation energy close to bulk self diffusion. In complete contrast to the findings of  
26 [5,6] in hexagonal zinc, they found for *fcc* aluminum that the mobility was always  
27 *independent* of tilt angle. Since the two sets of measurements were conducted in different  
28 angular ranges of misorientation and in different materials, the different misorientation  
29 dependence of mobility might be attributed to the different dislocation structures of the  
30 boundaries. Yang *et al.* [15] studied the mobility of low angle grain boundaries in  
31 aluminum at a single temperature,  $500^\circ\text{C}$ , using curvature as a driving force and found an  
32 essentially constant mobility for low angle boundaries, in agreement with the results of  
33 Winning *et al.*

34  
35  
36  
37  
38  
39  
40  
41  
42  
43  
44  
45  
46  
47  
48  
49  
50  
51  
52  
53  
54  
55  
56  
57  
58  
59  
60  
Lastly we note that the results show a singular transition from LAGB to HAGB behavior at  
a critical misorientation value [27]. The magnitude of this transition angle lies in the range  
8 to 14 degrees and varies according the crystallographic type of boundary. At first sight,  
reconciling this intrinsic structure dependent transition with a mobility that is controlled by  
extrinsic features of LAGBs is difficult. Note, however, that all mechanisms of LAGB  
migration involve diffusion of vacancies either in the vicinity of the boundary (where  
balanced vacancy exchange is possible) or through the bulk (where unbalanced vacancy  
flows control migration rates). The transition from LAGB to HAGB behavior may simply

1  
2  
3 mark the misorientation above which the internal structure of the boundary allows for more  
4 rapid transport of defects and diffusion in the bulk is no longer relevant.  
5  
6  
7  
8

## 9 10 **SUMMARY**

11 In summary, the experimental results for pure aluminum suggest that the mobility of  
12 LAGBs in the misorientation range between about  $3^\circ$  and  $15^\circ$  is essentially independent of  
13 misorientation angle. This suggests that the rate-controlling mechanism being that of climb  
14 of the intrinsic (structural) dislocations that bow out between pinning points of  
15 approximately constant density. The magnitudes of the observed activation energies  
16 suggest that diffusion of vacancies through the bulk is the rate-limiting step. A simple  
17 comparison of the theoretical mobility calculated with Eq. 30 and the measured value of  
18 mobility shows a difference in the order of one magnitude, which is probably based on the  
19 fact that most boundaries will have a smaller climb to glide ratio, and thus the actual  
20 mobility will be higher than the mobility in our simple estimation. Therefore the  
21 discrepancy is less serious than it might seem. We have examined a number of possible  
22 theories for the mobility of LAGBs and the only model that is able to explain the available  
23 facts is one in which the extrinsic dislocation content controls the mobility via their effect  
24 on pinning points for the intrinsic dislocations.  
25  
26  
27  
28  
29  
30  
31  
32  
33  
34  
35  
36  
37  
38

## 39 **ACKNOWLEDGMENTS**

40 ADR acknowledges the partial support of the MRSEC program of the National Science  
41 Foundation (Award Number DMR-0520425) and the hospitality of the Institute für  
42 Metallkunde und Metallphysik during a sabbatical period at the RWTH, Aachen in 2003.  
43 DJS gratefully acknowledges the support of the US Department of Energy (Grant No. DE-  
44 FG02-99ER45797). ADR and DJS also acknowledge the support of the Computational  
45 Materials Science Network, a program of the Office of Science, US Department of Energy.  
46 GG and LS gratefully acknowledge financial assistance from the Deutsche  
47 Forschungsgemeinschaft (Grant Go 335/10 and Grant Mo 848/7). The cooperation was  
48 supported by the Deutsche Forschungsgemeinschaft (DFG Grant 436 RUS 113/714/0-  
49 1(R)) and the Russian Foundation of Fundamental Research (Grant DFG-RRF1 03 02  
50  
51  
52  
53  
54  
55  
56  
57  
58  
59  
60



04000). MW gratefully acknowledges financial support from the Deutsche Forschungsgemeinschaft through the Heisenberg program (grant WI 1917/4).

### Appendix: *Climb of Extrinsic Dislocations via Pipe Diffusion*

An interesting alternative mechanism involving pipe diffusion exchange between extrinsic dislocations along the intrinsic (structural) dislocations also leads to a misorientation-independent mobility. Building on the analysis given for the basic pipe diffusion model in section 2.3, we assume the same driving force on the intrinsic dislocations given in Eqs. 3 and 4, and the same flux as given in Eq. 8, except that we now interpret the diffusion as taking place along the lines of the *intrinsic* dislocation lines. The total current of atoms resulting from pipe diffusion from one *extrinsic* dislocation to the next (per length of grain boundary) is

$$I = J_{\text{intrinsic}} \frac{\pi \delta_{\text{pipe}}^2}{d_{\text{intrinsic}}} \cong \frac{\tau}{kT} \left( \frac{\pi D_{\text{pipe}} \delta_{\text{pipe}}^2}{\lambda d_{\text{intrinsic}}} \right), \quad (\text{A1})$$

where  $\delta_{\text{pipe}}$  is the radius of the fast diffusion pipe at the (intrinsic) dislocation core and  $\lambda$  and  $d_{\text{intrinsic}}$  are the spacings between the extrinsic and intrinsic dislocations, respectively. The grain boundary velocity is then

$$v = I \frac{\Omega}{b} \cong \frac{\Omega}{kTb} \tau \left( \frac{\pi D_{\text{pipe}} \delta_{\text{pipe}}^2}{d_{\text{intrinsic}} \lambda} \right) \cong \frac{\Omega}{kTb} \left( \frac{\pi D_{\text{pipe}} \delta_{\text{pipe}}^2 \theta}{b \lambda} \right) \tau. \quad (\text{A2})$$

The mobility,  $M = v / (\tau \theta)$  with  $\Omega \sim b^3$ , is now simply

$$M \cong \frac{\Omega}{kTb} \left( \frac{\pi D_{\text{pipe}} \delta_{\text{pipe}}^2}{b \lambda} \right) \approx \frac{\pi \delta_{\text{pipe}}^2 b D_{\text{pipe}}}{\lambda kT}. \quad (\text{A3})$$

If this expression is compared with Eq. 7, it is evident that the mobility in this case is independent of the boundary misorientation. Provided that the extrinsic dislocation density does not vary, the mobility will be constant.

## REFERENCES

- 1  
2  
3  
4 [1] G. Gottstein and L.S. Shvindlerman, *Grain Boundary Migration in Metals*, (CRC  
5 Press, Boca Raton, 1999).  
6  
7 [2] Y. Huang and F.J. Humphreys, *Acta mater* **48** 2017 (2000).  
8  
9 [3] F.C. Frank FC, *Symposium on the plastic deformation of crystalline solids*, (Office  
10 of Naval Research, Pittsburgh, 1950) p.150.  
11  
12 [4] W. Read and W. Shockley, *Phys. Rev.* **78** 275 (1950).  
13  
14 [5] C.H. Li, E.H. Edwards, J. Washburn and E.R. Parker, *Acta metall* **1** 223 (1953).  
15  
16 [6] D.W. Bainbridge, C.H. Li and E.H. Edwards, *Acta metall* **2** 322 (1954).  
17  
18 [7] R. Viswanathan and C.L. Bauer, *Acta metall* **21** 1099 (1973).  
19  
20 [8] M. Winning, G. Gottstein and L.S. Shvindlerman, *Acta mater* **49** 211 (2001).  
21  
22 [9] M. Winning, G. Gottstein and L.S. Shvindlerman, *Acta mater* **50** 353 (2002).  
23  
24 [10] H. Luthy, A. Miller and O. Sherby, *Acta metall* **28** 169 (1980).  
25  
26 [11] J. Hirth and J. Lothe, *Theory of Dislocations*, (Wiley, 1982).  
27  
28 [12] D.A. Molodov, V.A. Ivanov and G. Gottstein, *Acta mater* **55** 1843 (2007).  
29  
30 [13] D.A. Molodov, T. Gorkaya and G. Gottstein, *Materials Science Forum* **558-559** 927  
31 (2007).  
32  
33 [14] T. Gorkaya, D.A. Molodov and G. Gottstein, *Intl. Conf. on Aluminum and its Alloys*  
34 editor: J. Hirsch (DGM, Aachen, 2008) p.1071.  
35  
36 [15] C.-C. Yang, A.D. Rollett and W.W. Mullins, *Scripta mater* **44** 2735 (2001).  
37  
38 [16] T. Furu, R. Ørsund and E. Nes, *Acta Metall Mater* **43**:2209 (1995).  
39  
40 [17] F.R. Boutin, *Journal de Physique* **C4.355** (1975).  
41  
42 [18] M. Peach and J.S. Koehler, *Phys. Rev.* **80** 436 (1950).  
43  
44 [19] H. Gleiter, *Phil. Mag* **20** 821 (1969).  
45  
46 [20] T.E. Volin, K.H. Lie and R.W. Balluffi, *Acta metall* **19** 263 (1971).  
47  
48 [21] A.P. Sutton and R.W. Balluffi, *Interfaces in Crystalline Materials*, (Clarendon  
49 Press, Oxford, 1995).  
50  
51 [22] W.T. Read, *Dislocations in Crystals*, (McGraw-Hill, New York, 1953).  
52  
53 [23] C.L. Bauer and M. Lanxner, *JIMIS-4* **27** 411 (1986).  
54  
55 [24] J.C.M. Li, *Electron Microscopy and Strength of Crystals*, editors G. Thomas and J.  
56 Washburn (Wiley & Sons, New York 1963) p.713.  
57  
58 [25] A. Lim, D.J. Srolovitz and M. Haataja, *Acta mater* **57** 5013 (2009).  
59  
60 [26] M. Biberger and W. Blum, *Phil. Mag. A* **65** 757 (1992).  
[27] M. Winning and A.D. Rollett, *Acta mater* **53** 2901 (2005).  
[28] M. Winning, *Adv. Solid State Phys.* **43** 563 (2003).

1  
2  
3  
4  
5  
6  
7  
8  
9  
10  
11  
12  
13  
14  
15  
16  
17  
18  
19  
20  
21  
22  
23  
24  
25  
26  
27  
28  
29  
30  
31  
32  
33  
34  
35  
36  
37  
38  
39  
40  
41  
42  
43  
44  
45  
46  
47  
48  
49  
50  
51  
52  
53  
54  
55  
56  
57  
58  
59  
60

**Table captions**

Table 1. Values used for estimate of mobility in aluminum.

Table 2. Values used for comparison of theoretical LAGB mobility with experiment.

Table 3. Summary of LAGB mobility mechanisms

For Peer Review Only

### Figure captions

Fig. 1. (a) Activation enthalpy plotted against misorientation for three series of grain boundary mobility experiments in aluminum. The misorientation axis for each series is noted in the legend. Note the constant activation enthalpy in both the low and high angle ranges, with a sharp transition between the low- and high-angle ranges. The mobilities are opposite to the enthalpies such that the mobility is low and constant in the low angle range and vice versa [28]. (b) Mobility at 400K plotted versus misorientation angle for symmetric tilt grain boundaries with  $\langle 100 \rangle$ ,  $\langle 111 \rangle$  or  $\langle 112 \rangle$  misorientation axes; note that the mobility is lower in the LAGB than in the HAGB range. (c) Mobility at 900K plotted versus misorientation angle, also for symmetric tilt grain boundaries with  $\langle 100 \rangle$ ,  $\langle 111 \rangle$  or  $\langle 112 \rangle$  misorientation axes; note that the mobility is lower in the HAGB range, in contrast to the behavior at 400K.

Fig. 2. (a) Dislocation structure in a low angle symmetrical tilt grain boundary; the dislocations are taken to be 110 lattice dislocations lying in the median lattice such that their Burgers vectors are perpendicular to the 110 boundary plane normal. (b) Structure with the grain boundary displaced to the right.

Fig. 3. Geometry of glide in a low angle grain boundary: arrangement of edge dislocations in a symmetric tilt grain boundary gliding on nearly parallel planes.

Fig. 4. Diffusion between dislocations of opposite sign within a rigid grain boundary. Here the dislocations are distributed equally between the two lattices on either side of the grain boundary.

Fig. 5. Structure of an asymmetric tilt grain boundary.

Fig. 6. Diffusion between dislocations of opposite sign within a flexible grain boundary.

Fig. 7. Schematic illustration of a unit cell for the low-angle symmetric grain boundary, as constructed from uniformly spaced parallel dislocations  $\mathbf{b}_1 = 110$ , in the presence of parallel

1  
2  
3 extrinsic dislocations  $\mathbf{b}_2=1-10$  and  $-\mathbf{b}_2=-110$ . The unit cell is only repeated along the  $y$ -  
4 direction, i.e., there are no periodic images along the  $x$ -direction.  
5  
6  
7

8  
9 Fig. 8. This shows four dislocation configurations for migration, based on the structure  
10 shown in the previous figure, with a climb mobility equal to 0.2 of glide mobility under  
11 applied stress  $\sigma_{xy} = 4 \times 10^{-3}$  in units of shear modulus. The boundary moves from left to  
12 right. Below the threshold stress at finite climb mobility, the boundary drags along the  
13 extrinsic dislocations (labeled as  $\pm \mathbf{b}_2$ ) as it migrates.  
14  
15  
16  
17  
18  
19  
20  
21  
22  
23  
24  
25  
26  
27  
28  
29  
30  
31  
32  
33  
34  
35  
36  
37  
38  
39  
40  
41  
42  
43  
44  
45  
46  
47  
48  
49  
50  
51  
52  
53  
54  
55  
56  
57  
58  
59  
60

1  
2  
3 **Table captions**  
4  
5  
6  
7  
8  
9  
10  
11  
12  
13  
14  
15  
16  
17  
18  
19  
20  
21  
22  
23  
24  
25  
26  
27  
28  
29  
30  
31  
32  
33  
34  
35  
36  
37  
38  
39  
40  
41  
42  
43  
44  
45  
46  
47  
48  
49  
50  
51  
52  
53  
54  
55  
56  
57  
58  
59  
60

---

For Peer Review Only

1  
2  
3  
4  
5  
6  
7  
8  
9  
10  
11  
12  
13  
14  
15  
16  
17  
18  
19  
20  
21  
22  
23  
24  
25  
26  
27  
28  
29  
30  
31  
32  
33  
34  
35  
36  
37  
38  
39  
40  
41  
42  
43  
44  
45  
46  
47  
48  
49  
50  
51  
52  
53  
54  
55  
56  
57  
58  
59  
60

For Peer Review Only



<i>Parameter</i>	<i>Value</i>
$\gamma_0$	324 mJ/m <sup>2</sup>
$D_L$	$1.76 \cdot 10^{-5} e^{-Q/RT}$ (m <sup>2</sup> /s), $Q=126.1$ kJ.mol <sup>-1</sup>
$D_{\perp}$	$2.8 \cdot 10^{-6} e^{-Q/RT}$ (m <sup>2</sup> /s), $Q=81.9$ kJ.mol <sup>-1</sup>
$b$	0.286 nm
$\delta$	0.286 nm
$\Omega$	$16.5 \cdot 10^{-30}$ m <sup>3</sup>
$\alpha$	1

Table 1

<i>Parameter</i>	<i>Value</i>
$D_L$	$10^{-13} \text{ m}^2 \cdot \text{s}^{-1}$ (at 800K)
$\delta$	$3b \approx 0.858 \text{ nm}$
$kT$	$1.1 \cdot 10^{-20} \text{ J}$ (at 800K)

Table 2

For Peer Review Only

	<i>Structure</i>	<i>Main Assumption</i>	<i>Driving Force</i>	<i>Temperature Dependence</i>	<i>Mobility Dependence on Misorientation</i>
1	Symmetrical tilt 1 Burgers vector	Dislocation glide	Stress	Weak (as for plastic deformation)	Independent of misorientation
2	General LAGB + extrinsic dislocations	Dislocation climb; diffusion of vacancies between extrinsic dislocations	Stress or curvature	Same as for bulk diffusion	Decreases as $1/\theta$
3	Symmetric tilt + twist component	Dislocation climb; vacancy exchange between dislocations	Stress or curvature	Same as for pipe diffusion (along dislocations)	Decreases as $1/\theta$ and depends on twist angle
4	Symmetric tilt, 2 Burgers vectors	Dislocation climb; vacancy exchange between adjacent dislocations	Stress or curvature	Same as for bulk diffusion of vacancies	Independent of misorientation
5	Asymmetric tilt	Climb of intrinsic dislocations; vacancies from/to bulk	Stress or curvature	Same as for bulk diffusion	Decreases as $1/\theta$
6	Flexible, general LAGB + pinning points	Climb of extrinsic pinning points; vacancies from/to bulk	Stress or curvature	Same as for bulk diffusion	Independent of misorientation

Table 3

Fig. 1a

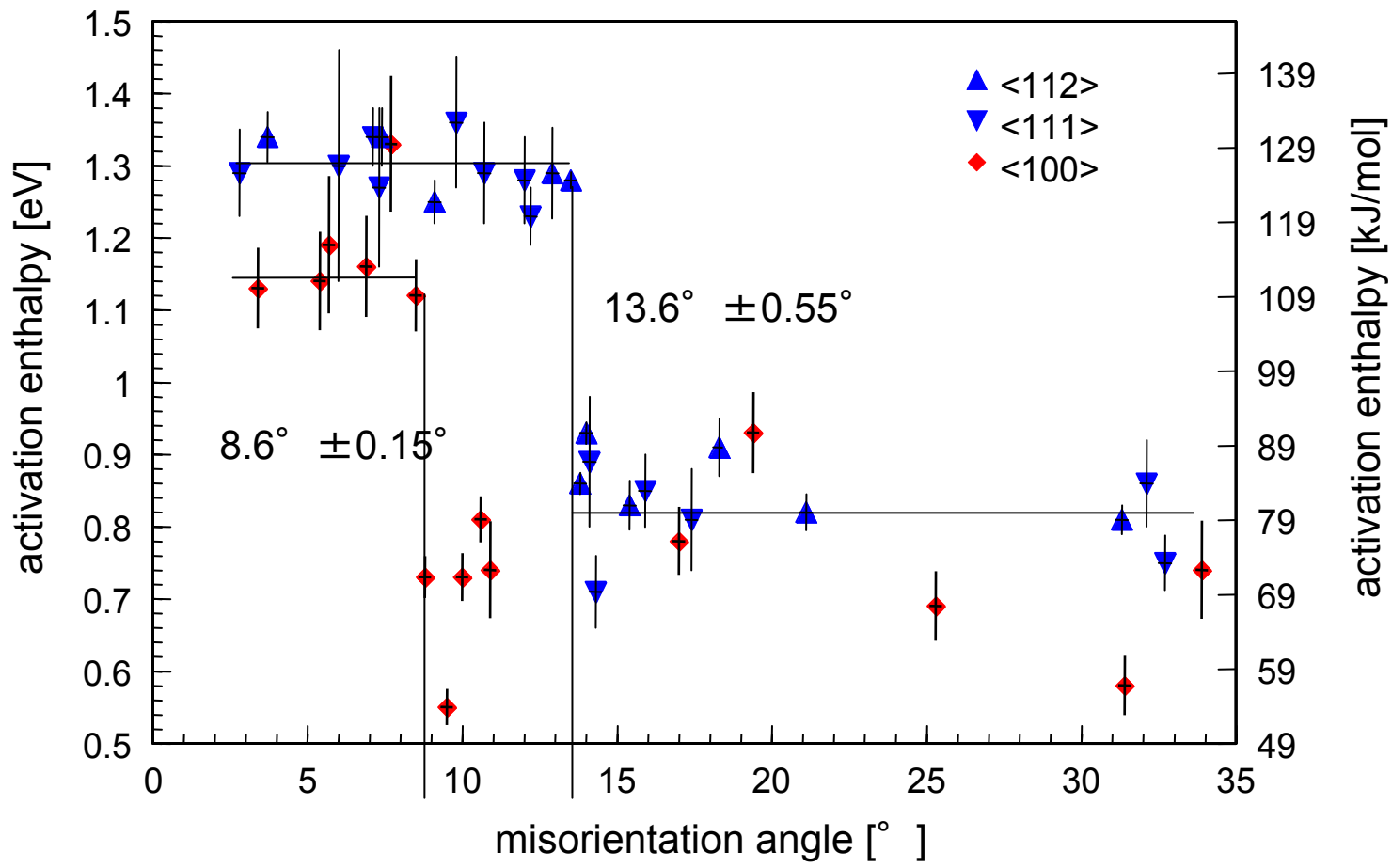


Fig. 1b

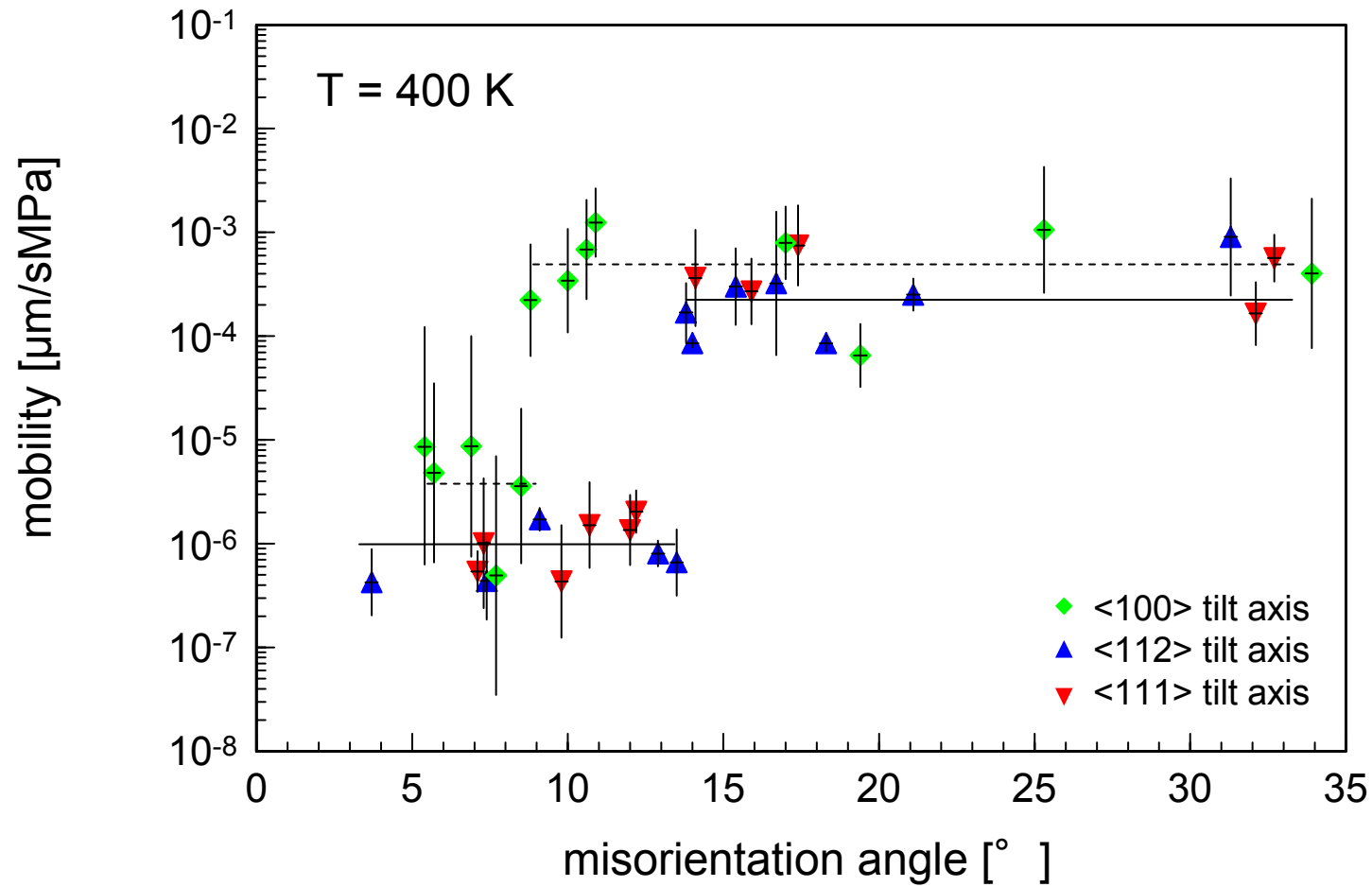


Fig. 1c

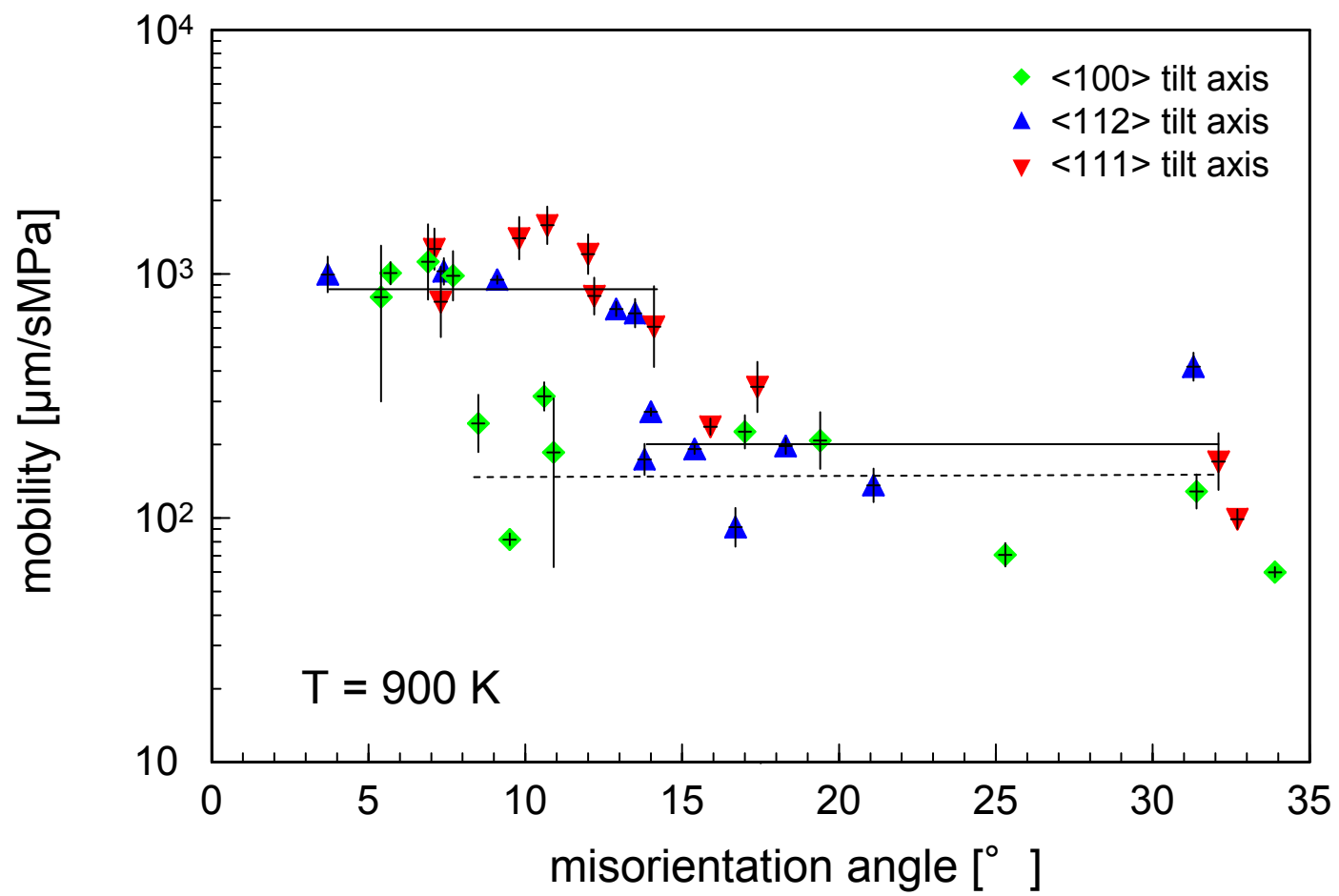


Fig. 2a

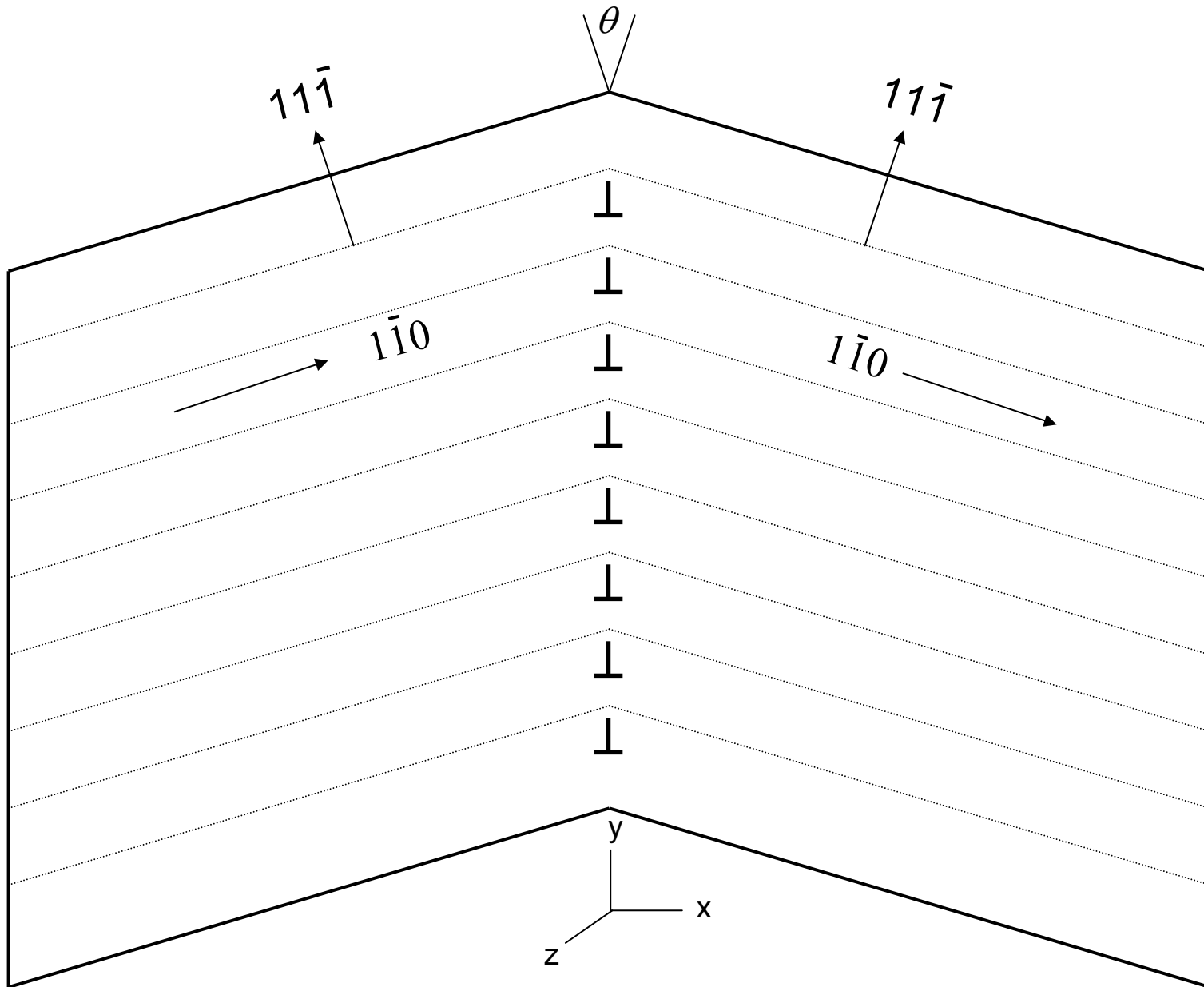




Fig. 2b

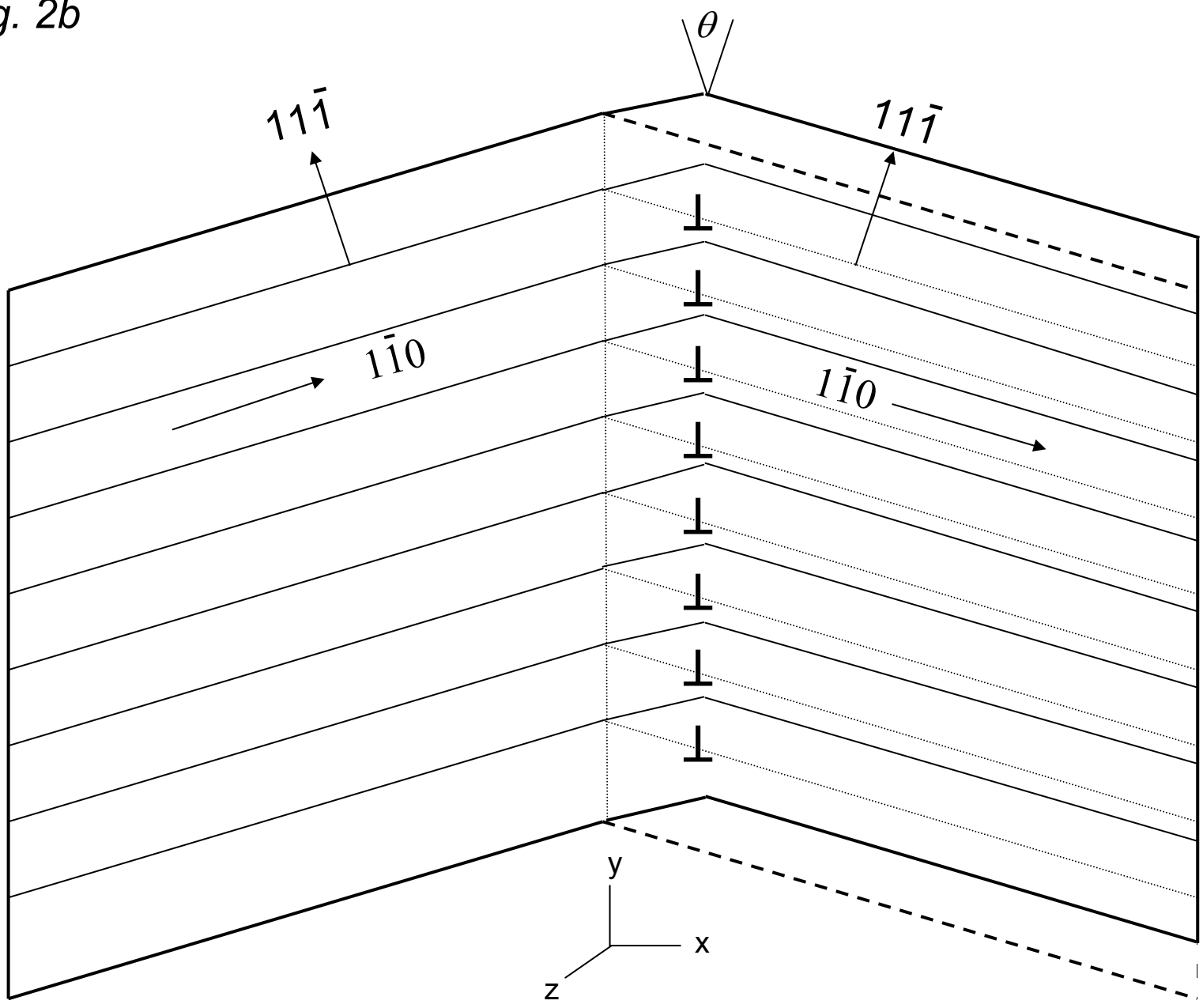
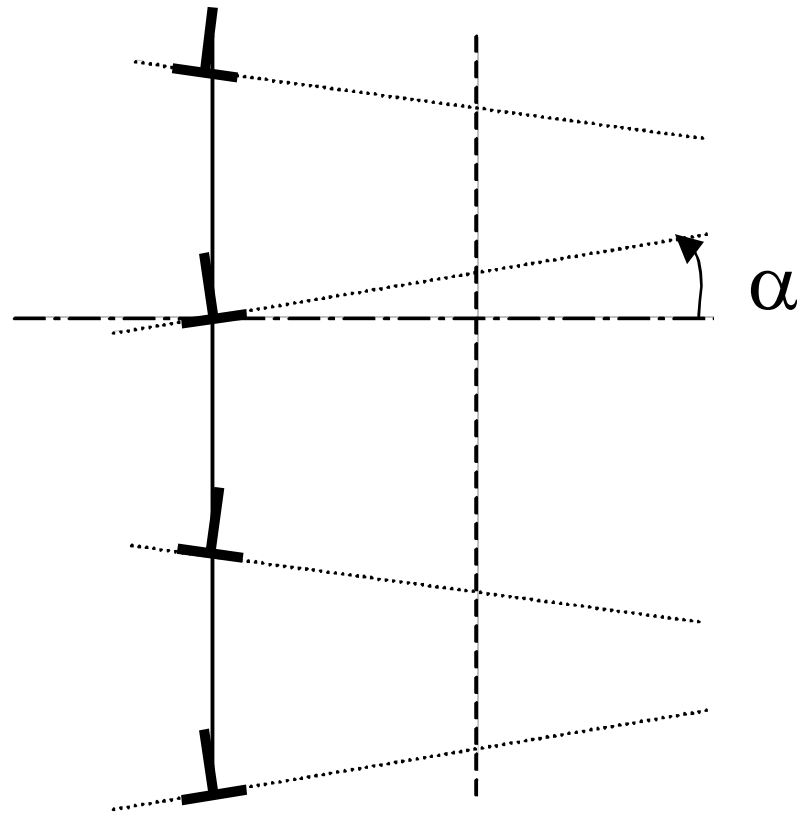


Fig. 3



1  
2  
3  
4  
5  
6  
7  
8  
9  
10  
11  
12  
13  
14  
15  
16  
17  
18  
19  
20  
21  
22  
23  
24  
25  
26  
27  
28  
29  
30  
31  
32  
33  
34  
35  
36  
37  
38  
39  
40  
41  
42  
43  
44  
45  
46  
47  
48  
49

Fig. 4

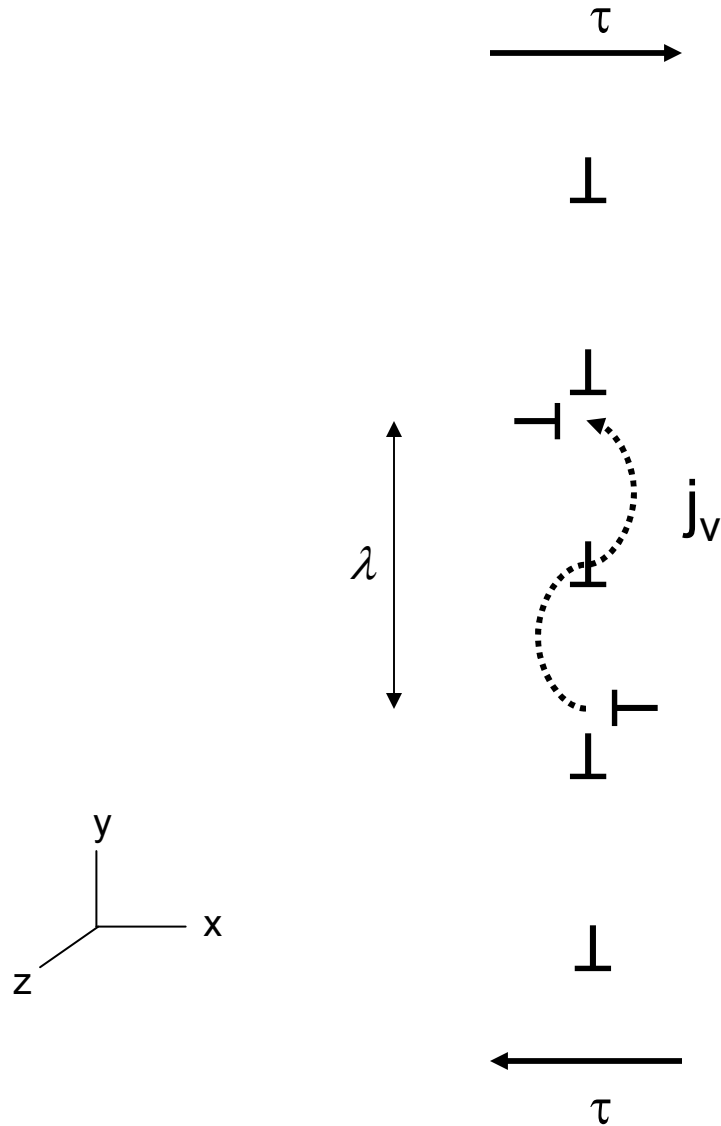
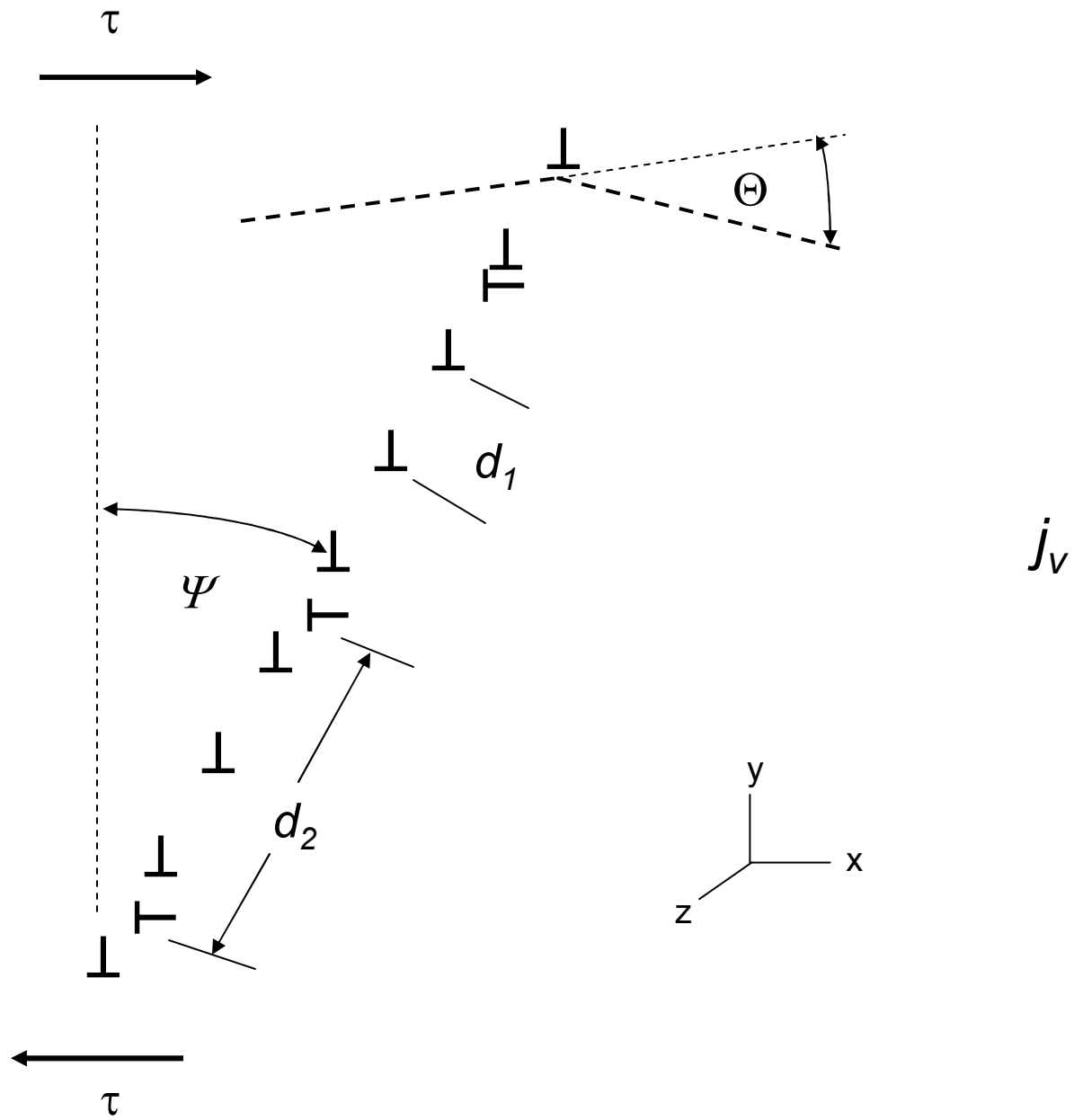


Fig. 5



1  
2  
3  
4  
5  
6  
7  
8  
9  
10  
11  
12  
13  
14  
15  
16  
17  
18  
19  
20  
21  
22  
23  
24  
25  
26  
27  
28  
29  
30  
31  
32  
33  
34  
35  
36  
37  
38  
39  
40  
41  
42  
43  
44  
45  
46  
47  
48  
49

1  
2  
3  
4  
5  
6  
7  
8  
9  
10  
11  
12  
13  
14  
15  
16  
17  
18  
19  
20  
21  
22  
23  
24  
25  
26  
27  
28  
29  
30  
31  
32  
33  
34  
35  
36  
37  
38  
39  
40  
41  
42  
43  
44  
45  
46  
47  
48  
49

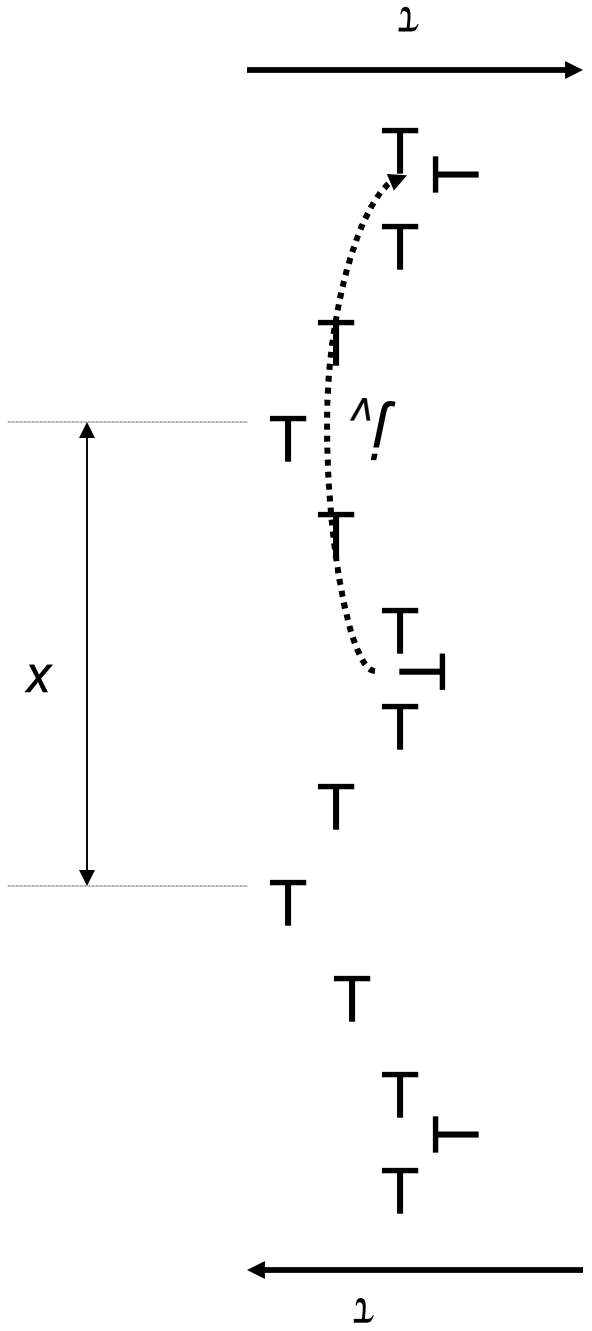


Fig. 6

Fig. 7

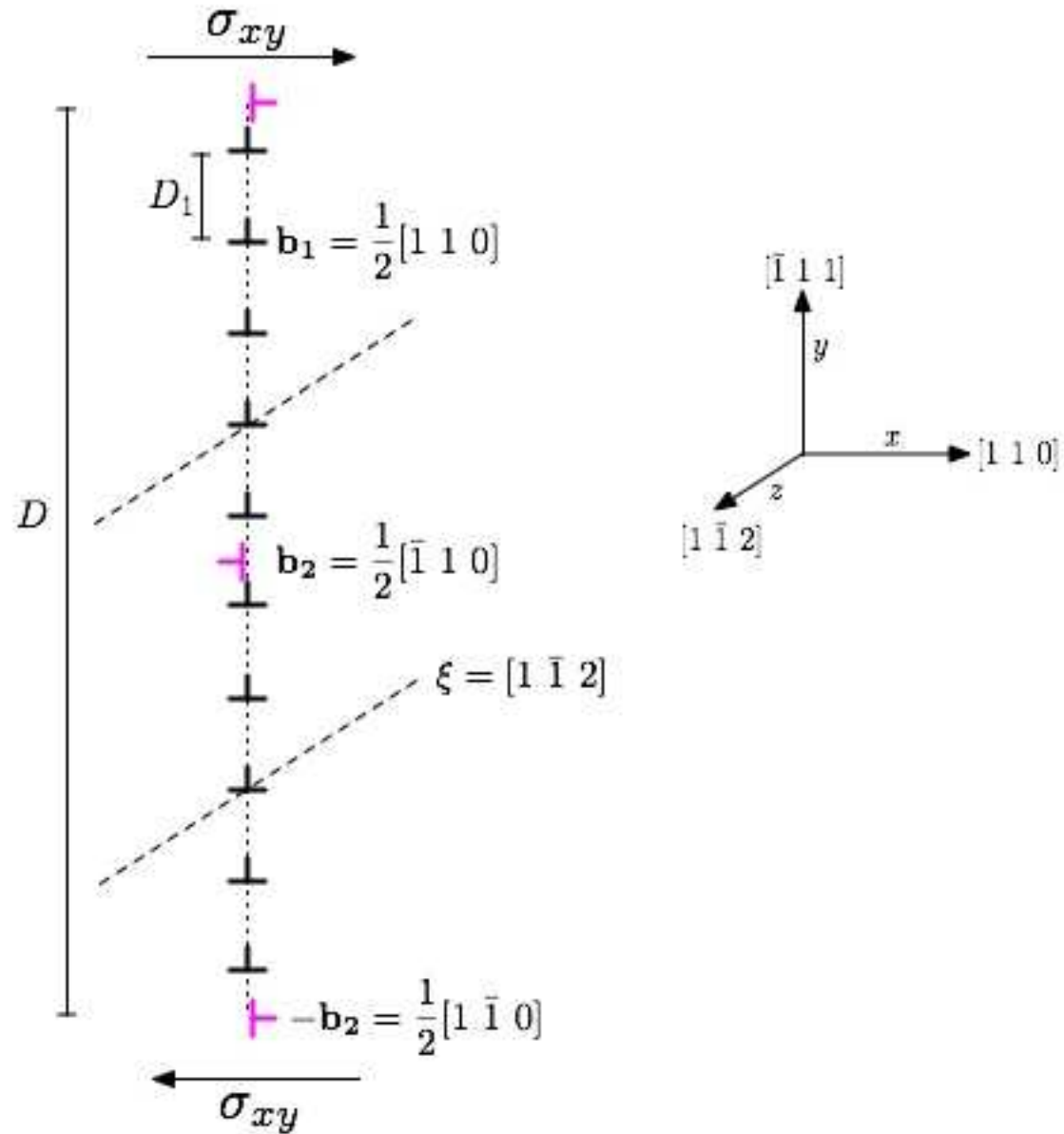


Fig. 8

